

# Rapport d'activité

## Etude de la génération de séismes et la propagation des ondes sismique

- Study on the earthquake generation and seismic wave propagation processes -

### 1. General Information

**Projet :** A0070406700

**Responsable :** AOCHI Hideo

#### Allocation

CINES BULL noeuds fins Occigen : 155 000 heures scalaires

#### Consommation

CINES BULL noeuds fins Occigen : 147 609 heures scalaires, soit 95.2% par rapport à 79.78% de temps passé (18/08/2020)

### 2. Scientific Results (below is written in English)

Since November 2019, we have been focusing both on dynamic simulation and kinematic modeling of the 2015 Mw8.3 Illapel (Chile) earthquake, using Boundary Integral Equation Method (BIEM) and Finite Difference Method (FDM). The result had been submitted to JGR in April 2020, however some numerical verification tests were demanded. We have been working on the supplementary simulations and verification tests and the paper is going to be resubmitted soon (**Aochi and Ruiz, firstly submitted to JGR in April 2020**).

Our kinematic modeling proposes two-step rupture process of the 2015 Illapel earthquakes, namely the first rupture ends with magnitude of 6.9 at maximum without triggering the main rupture of magnitude 8.3 and a second nucleation is required at depth delayed by up to 20 seconds. We have reconstructed dynamic rupture model considering the seismicity and interseismic coupling (**Figure 1**). To arrive there, we have carried out different numerical simulations through the assimilation with the observed and synthetic data.

- 1) In order to justify the inversion process of kinematic rupture, we held numerical inversion test, namely, to reconstruct the given source mode dynamically simulated with kinematic description. **Figure 2** illustrates the comparison of two models, each of which is dynamically simulated, and then inverted by two patch models. Here, the synthetic ground motions of dynamic rupture models and Greens' functions for the inversion are calculated in the same way using a finite difference method (FDM). It is also worth noting that there have been few

cross-checking studies (to my knowledge) on dynamic rupture simulations and kinematic inversions. In short, the used kinematic description (much simplified “patch” models instead of the usual finite source model by subfault) is able to identify the main asperity (slip area) with another small one close to the epicenter both spatially and temporally. Nevertheless, the simplification of “patch” model provides only one characteristic feature for a given frequency, so that it may underestimate (smoothen) the process when the rupture process becomes complex (Model 3 in panel (d)). However this simplified inversion process is rapid enough to outline fast the finite source parameters of a large earthquake.

- 2) The estimation of the frictional parameters has been studied thorough dynamic rupture simulations and comparison with the observed data. **Figure 3** illustrates model geometry of the fault and the calculated misfit between the synthetic and observed ground motions at 10 continuous GPS stations (0.01 – 0.05 Hz). The result is shown in function of parameter  $\kappa$ , an indicator of rupture process, physically indicating the ratio of the available strain energy to the energy release rate coupled with a slip-weakening friction law. The shadow area does not allow the rupture progress on the main patch. As a result, it is found that the preferred situation is that the stress field is just sufficient but not too much. The fracture energy is estimated as 7.5 MJ/m<sup>2</sup>, which follows the scaling relation of earthquake dynamics previously found by different researchers (also summarized in **Aochi & Twardzik, Pageoph, 2020**; which was the result of the last year).

Typical dimension of the dynamic rupture modeling using BIEM is 175 km x 130 km (reduced resolution of a fault element of 1 km, namely about 20 000 elements; this is a limit for many simulations) and for FDM a volume of 300 km x 450 km x 50 km (still reduced resolution of grid of 500 m, namely 54 million grids, but this is enough for discussing very low-frequency behaviors). **Although such low-resolution modeling was sufficient for many simulations of our purpose, high-resolution model is required to realize complex rupture process more in detail and ground motion at higher frequencies. This will be a subject of the coming year.**

Besides the main topics presented above, we had an occasion to re-discuss the multi-scale heterogeneous rupture model (**Figure 4**) for different points of view. In particular, Julien Renou (PhD thesis defended at IGP in January 2020) statistically analyzed the dynamically simulated rupture models and show the coincidence of the acceleration appearing in source time function with the observational data. We think this is an important study showing that there is always an acceleration phase of rupture process of an earthquake from the observations and this corresponds well to the dynamic rupture simulation supposing multi-scale heterogeneity of fracture energy on a fault. This study was presented briefly at EGU online this year and hopeful will be summarized as a scientific paper very soon. Such discussion will be helpful to develop the dynamic rupture models in high frequencies (see above).

Another contribution is carried out particularly for the wave propagation in 3D medium. **Figure 5** demonstrates the realization of the 2016 Mw3.9 Lacq (SW France)

earthquake around the depleted gas reservoir of Lacq basin. The lateral heterogeneity is strong enough to perturb the wave propagation. This ‘felt earthquake’ has a mechanism of normal faulting, consistent with the stress field above the depleted reservoir. We are also studying the 2020/06/03 ML3.6 (Mw3.6) earthquake which took place in the East of Lacq basin. This earthquake implies instead a strike-slip faulting, probably a tectonic event. But this should be scrutinized with the effect of 3D structure. The calculation is a dimension of 30 km x 30 km x 15 km only, but with a 120 million elements to arrive higher frequencies. This is a contribution to the H2020 GEOERA- HIKE project (Mid-term progress report, Nov 2019). The final result of this study will be published, hopefully in 2021.

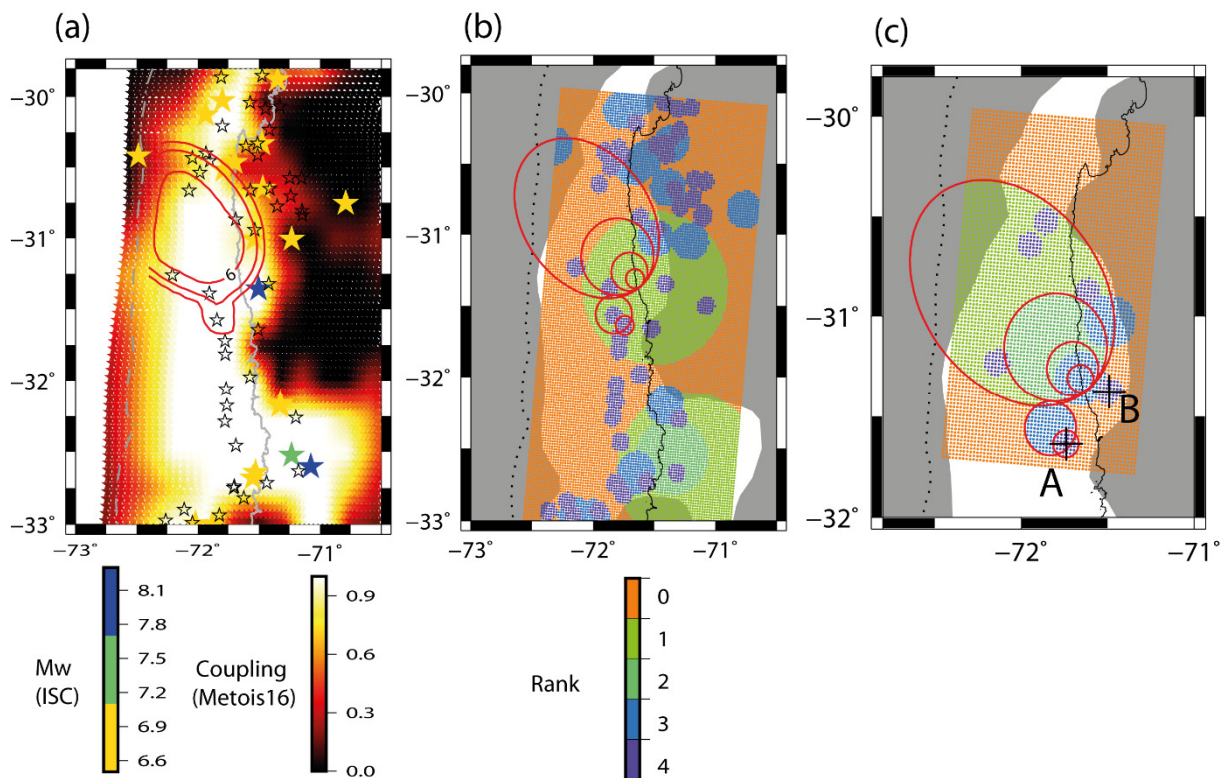


Figure 1 : (a) Slip distribution (every 2 m) from the preferred dynamic simulation (Figure 14a). The maximum slip is 7.99 m, corresponding to Mw8.16. The earthquakes (stars) are based on the bulletin of International Seismological Centre (ISC) for the period of 1904 – 2014, colored differently for each magnitude range of  $M_w > 7.7$ ,  $7.7 \geq M_w > 7.1$ ,  $7.1 \geq M_w > 6.5$  and the others in open stars ( $6.5 \geq M_w > 6.0$ ). Note that the largest one Mw8.1 occurred on 1943/04/06 and no earthquakes are reported for the second range of magnitude around the Illapel earthquake. The background represents the coupling obtained by Métis et al. (2016). The color scale is reversed from the original figure, so as to emphasize strong coupling area with large coseismic slip. (b) The attributed patch distribution corresponding to each earthquake in color. The shaded area represents the coupling coefficient smaller than 0.7. The dynamic rupture model obtained in the previous section is illustrated in red lines. (c) Adopted dynamic rupture model for the final simulation in color scale. The largest patch and neighboring are shifted so as to fit the previously obtained patch position.

The points A and B denote the first and second nucleation points in the simulation. (Aochi and Ruiz, 2020)

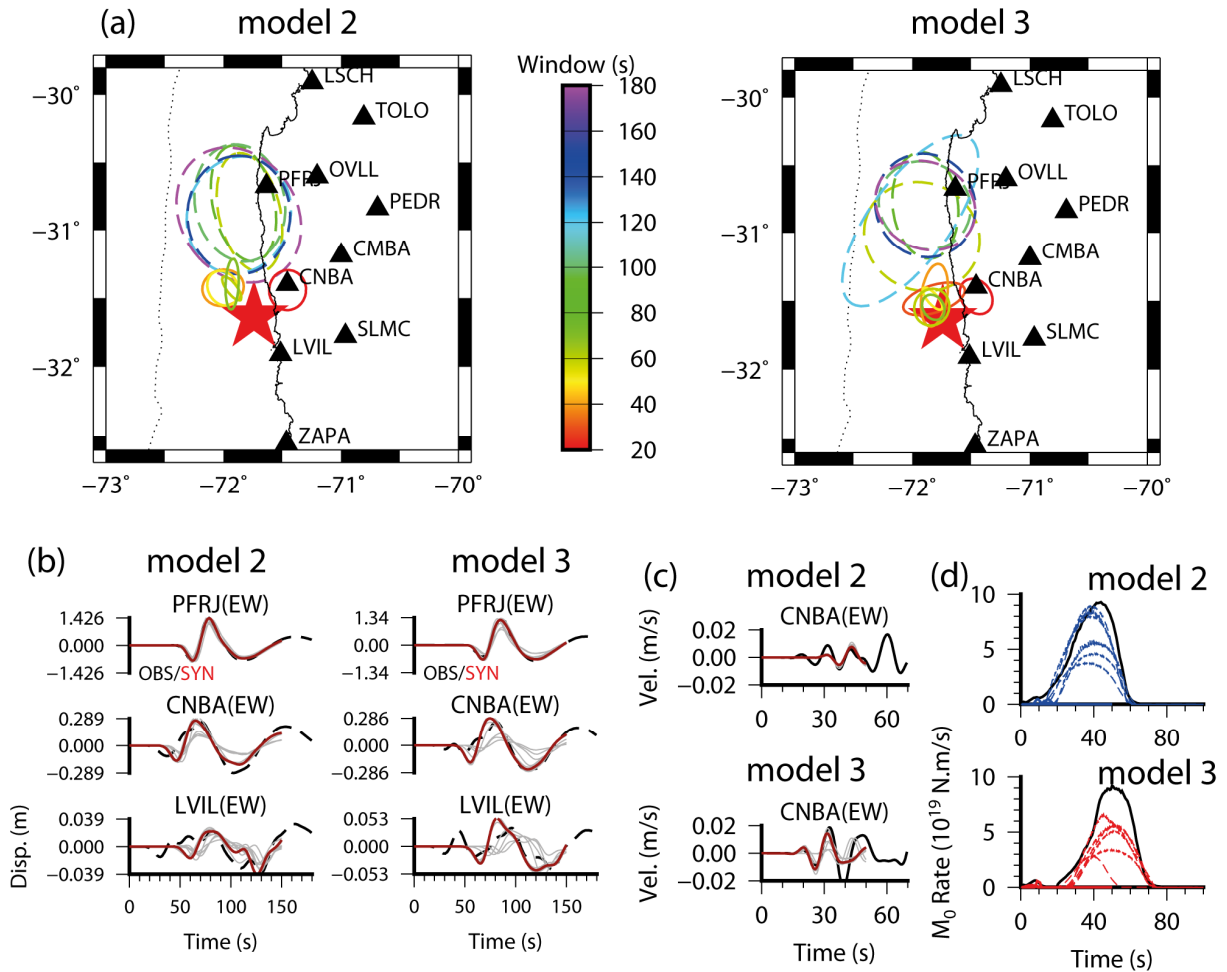


Figure 2: Synthetic inversion results for Models 2 and 3, which are previously dynamically simulated using BIEM. (a) Obtained patch geometry in function of time windows. The broken and solid lines represent two inversion processes of the large scale and the early stage equivalent to the previous analyses. (b) An example of the comparison of ground motions at the selected stations for the large scale inversion (displacement in 0.01-0.05 Hz, time window of 150 s). The grey lines show the intermediate solutions during the inversion. (c) A comparison of ground motions at CNBA (velocity in 0.03 – 0.1 Hz, time window of 50 s). (d) Comparison of source time function (rate of seismic moment release  $M_0$ ). All the solutions for different time windows are shown. (Aochi & Ruiz, 2020)

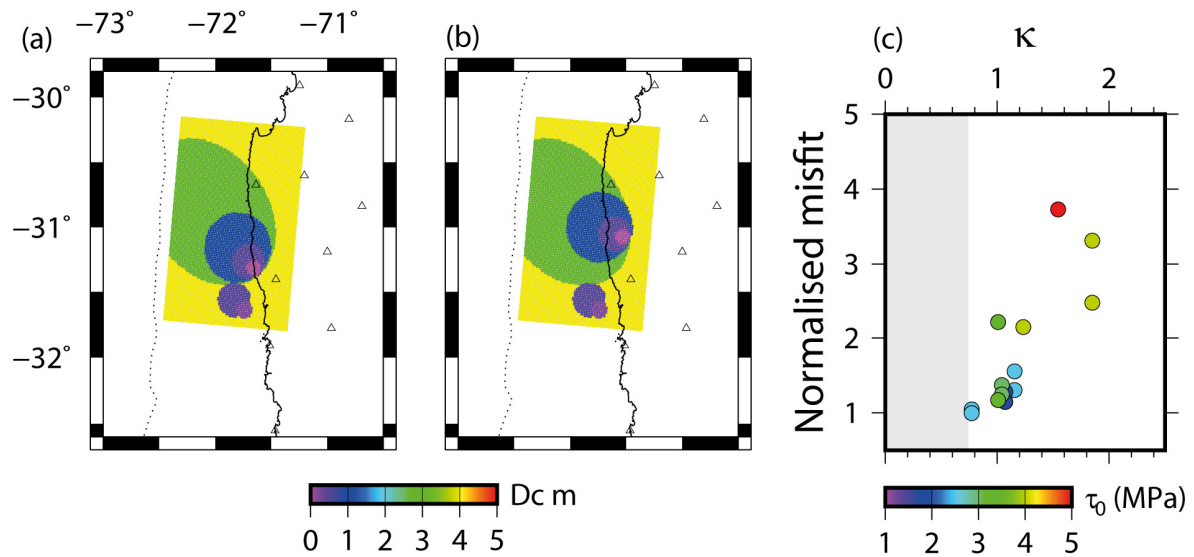


Figure 3 : (a, b) Two examples of model parameter distribution ( $D_c$ ) and two nucleation points. (c) Misfit in function of parameter  $\kappa$  and initial stress level  $\tau_0$ . In grey zone ( $\kappa < 0.741$ ), the large patch is not ruptured. (Aochi & Ruiz, 2020)

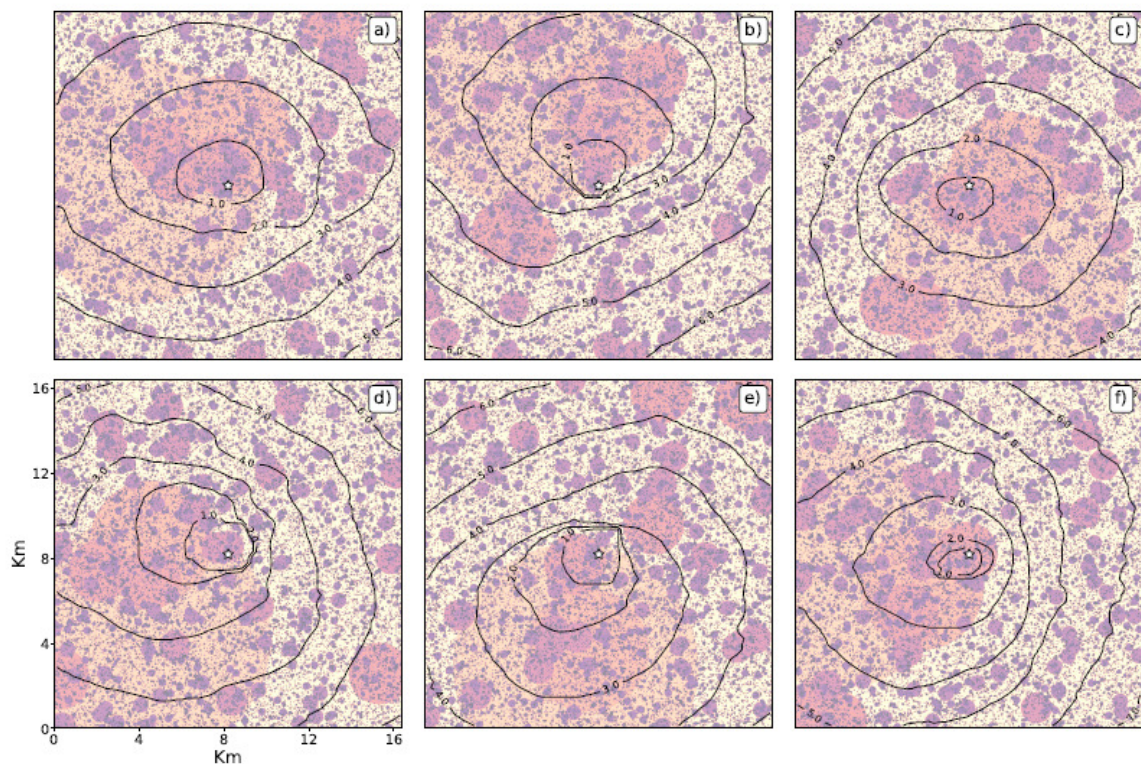


Figure 4: Representation of six fault heterogeneity maps from a random circular patches position (colored differently according to size). White star is the position of the hypocenter. Black lines show the contours of the rupture front every second simulated using BIEM. (Renou et al., EGU, 2020)

# 2016/04/25 ML4.0 (Mw3.9) Lacq earthquake

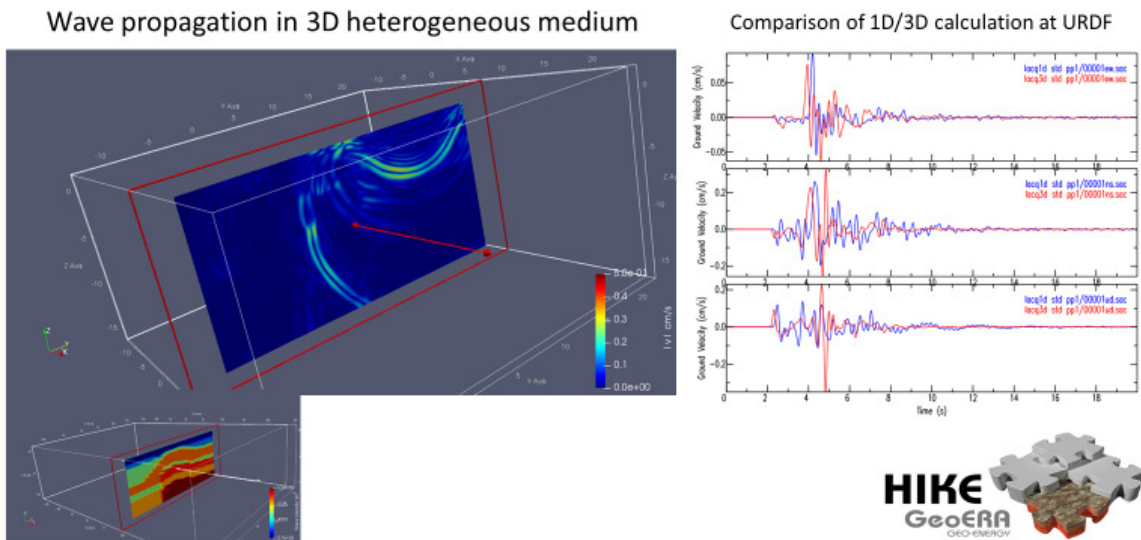


Figure 5: Regional study on the comparison of ground motion in 1D/3D structure models around the Lacq (SW France) area. (Presentation material in November 2019).

## 3. Publications submitted or in preparation

Aochi, H. and C. Twardzik, Imaging of seismogenic asperities of the 2016 ML6.0 Amatrice, Central Italy, earthquake through dynamic rupture simulations, Pageoph, 170, 1931-1946, doi:10.1007/s00024-019-02199-z, 2020.

Aochi, H. and S. Ruiz, Early stage and main megathrust rupture of 2015 Mw 8.3 Illapel, Chile, earthquake from kinematic inversions and dynamic simulations, submitted to J. Geophys. Res., April, 2020 (to be resubmitted in September 2020)

## 4. Conferences and posters

Aochi, H. and S. Ruiz, Kinematic and dynamic modeling of the 2015 Mw8.3 Illapel, Chile, earthquake AGU Fall Meeting, San Francisco, USA, December 2020.

Renou, J., M. Vallée and H. Aochi, Observations and modeling of the rupture development based on the analysis of Source Time Functions, EGU General Assembly, Abstract 9557. (with online presentation)

Ide, S. and H. Aochi, Hierarchical seismic source model and recent observational evidence, EGU General Assembly, Abstract 11916. (abstract only)